MSc in Photonics

PHOTONICS**BCN**

Universitat Politècnica de Catalunya (UPC)
Universitat Autònoma de Barcelona (UAB)
Universitat de Barcelona (UB)
Institut de Ciències Fotòniques (ICFO)

http://www.photonicsbcn.eu

Master in Photonics

MASTER THESIS WORK

Plasmon Enhanced Chirality

Jose García Guirado

Supervised by Dr. Romain Quidant, (ICFO)

Presented on date 19th July 2013

Registered at

Escola Tècnica Superior d'Enginyeria de Telecomunicació de Barcelona

Plasmon Enhanced chirality

Jose García Guirado

ICFO - The Institute of Photonic Sciences, Av. Carl Friedrich Gauss, num. 3 08860 Castelldefels (Barcelona), Spain

E-mail: jose.garcia@icfo.es

Abstract. An experimental set-up to measure plasmon-enhanced Circular Dichroism (CD) on Planar Chiral Metamaterials (PCM) has been designed, built and tested. PCM, made of two-dimensional arrays of metallic nano-particles, have been fabricated and their geometry optimized to maximise their CD response. We carried out first test experiments on N-Isobutyryl-Cysteine molecules in both enantiomeric forms, and observed a clear sensitivity to the handiness of the molecules.

Keywords: Chirality, chiral nanostructures, Circular Dichroism, localized surface plasmon

1. Introduction

Most of biomolecules, such as sugars, amino acids and proteins, are chiral, i.e. they can not be superimposed to their mirror image. The two mirror images are named enantiomers. Usually only one of the enantiomers can be found in nature. However, when these molecules are synthetized, both enantiomers are generated, and are not distinguishable by structural analysis techniques. Fortunately, each enantiomer interact differently with circular polarized light; D (Dextrorotatory) enantiomer absorbs more Right handed Circularly Polarized light (RCP), and L (Levorotatory) enantiomer absorbs more Left handed Circularly Polarized light (LCP) [1]. The different absorption between RCP and LCP of a specimen is known Circular Dichroism (CD).
Because enantiomers can have very different biochemical behaviour, it is crucial to be able to discriminate them. For example they can smell or taste different; more importantly, one enantiomer can be a beneficial drug and the other a poison [2]. Chemical and pharmaceutical industry already have developed analytical methods based on Optical Rotatory Dispersion (ORD) and CD, however the low chiroptical activity of individual molecules limits the sensitivity of devices to macroscopic samples. Moreover the CD peaks of these molecules are typically in Ultraviolet (UV) region which adds technical issues and increases the cost of devices [3, 4].
Plasmonic nanoparticles have the properties to localize and enhance the electromagnetic (EM) field [5]. Localized Surface Plasmon Resonances (LSPR) can be tuned by

controlling the size, shape, and the material of nanoparticles. LSPR are very sensitive to changes in its environment, and thus can be used to detect small amounts of molecules. More recently, it was demonstrated that plasmonic nanoparticles can also be designed to discriminate chiral molecules [6, 7].
In this work, a platform to measure plasmon-enhanced CD was designed and mounted. For validation, the platform was tested on PCM to measure the handiness of the nanostructures. Finally, we successfully demonstrated discrimination of chiral molecules by plasmon-enhanced CD measurements on PCM.

1.1. Circular dichroism

Circular polarized light can be described by the combination of two linear polarized waves of same frequency and amplitude, and perpendicular electric vectors with a relative phase difference of $\pm\pi/2$. Commonly these states with relative phase $\pm\pi/2$ are called Left and Right Circularly Polarized light (LCP, RCP) [8].
CD is by definition the difference between the absorbance of RCP and LCP [9]:

$$CD = A_R - A_L \tag{1}$$

Two enantiomers having opposite chiroptical properties, show opposite CD sign.

1.2. Chiral plasmonic nano structures

Several experiments have been reported in the literature, showing CD peaks in the visible frequency range, from complexes formed by chiral molecules attached to colloid metallic nanoparticles [10, 11].
In contrast M. Kadodwala and coworkers [12] show the viability of a system based on Right and Left Handed PCM (RHPCM and LHPCM) which allows the discriminations of proteins featuring β-sheets and α-helices. The detection principle is based on monitoring changes in the CD spectrum of the nanostructures. The chiral structures they used (so called Gammadions) are based on Schwanecke et al. and Kuwata-Gonokami et al. previous experiments [13, 14].

Based on Kadodwala's experiment, we have developed a CD spectrometer compatible with PCM. The work developed here is mostly experimental, and our primary aim was to build the set-up and software for instrumentation control, as well as testing it for the discrimination of enantiomers.

2. Methods

2.1. Experimental set-up

The experimental set-up consists of an optical transmission spectroscopy set-up. The ilumination of the sample alternates between RCP and LCP light.
Figure 1 shows a simplified block diagram and a photo of the experimental set-up that

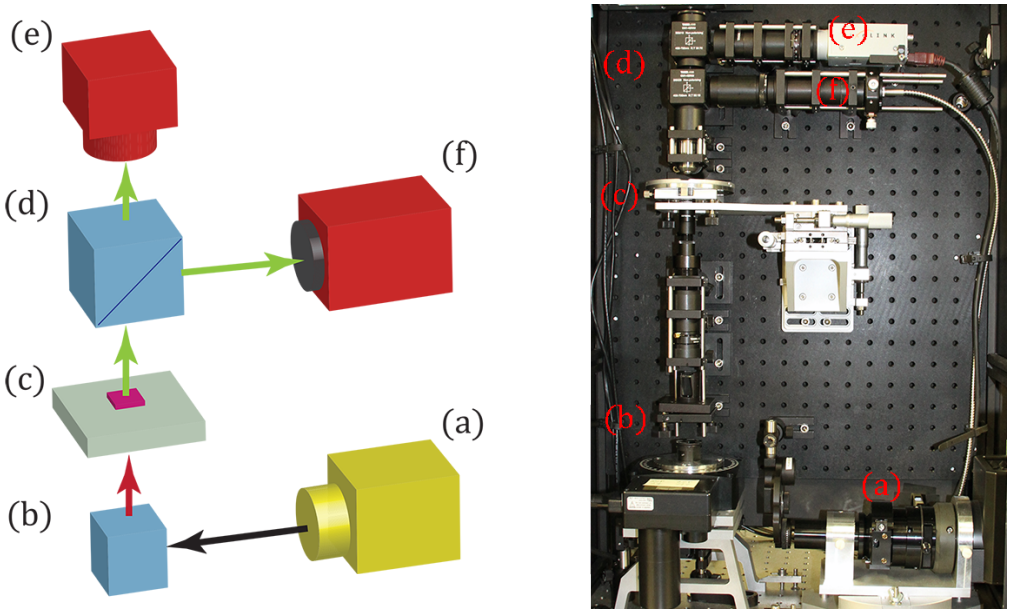

Figure 1. Left: Block diagrams of the main parts of the experimental set-up. Right: Photography of the experimental set-up. (a) white light source, (b) circular polarizer sub-system, (c) sample plane, (d) beam-splitter, (e) CCD camera, and (f) spectrometer.

we have developed. Incoherent white light is circularly polarized by a linear polarizer prism and quarter wave prism. Rotating the linear polarizer changes the handiness of circular polarization. The sample is placed in a specially designed support which allows the sample scanning over an area of 25×25 mm^2, and focusing. A low numerical aperture ($NA = 0.25$) and magnification objective ($10\times$) collects the light, and a beam-splitter divides the beam into the two detection paths, one for the imaging CCD camera for large field of view, and the other with small collection region ($\oslash = 50\,\mu$m) for the spectrometer.

2.2. Numerical simulations

Using RF module of Comsol 3.5a multiphysics software, we perform numerical simulations of the EM response of the PCM structures to RCP and LCP light. The CD spectra have been calculated for both PCM. Figure 2 shows the normalized near field electric field intensity distribution for Left handed gammadion excited with LCP (a) and RCP (b) light of wavelength 860 nm. The coupling of LCP light to the gammadion is stronger than with RCP light, the near-field map shows strong interaction between the arms of gammadion excited with LCP. Figure 2 (c) shows the CD spectra of right and left handed PCM. As expected the CD spectra are found to be of opposite signs.

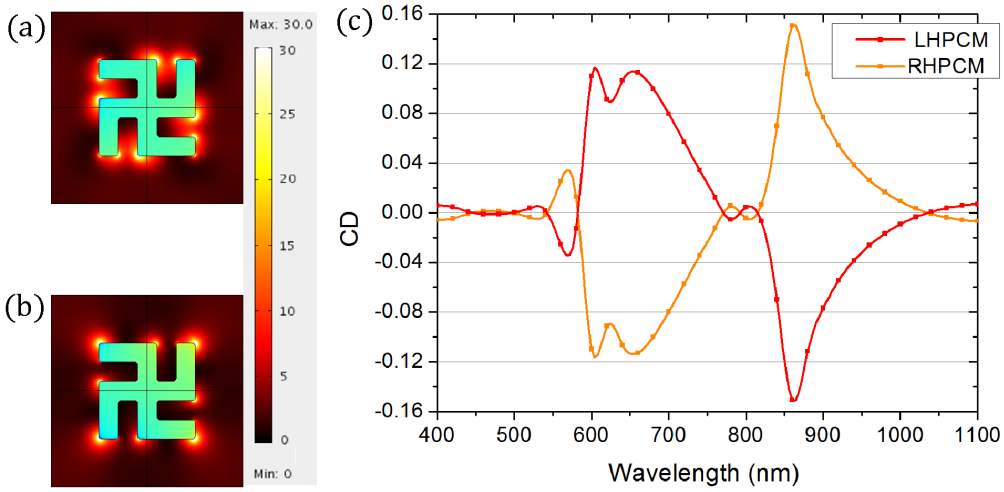

Figure 2. FEM calculations of the optical near-field of left handed gammadions (a) exited with LCP and (b) with RCP light of wavelength 860 nm. The near-field interaction between legs of the gammadion enhances the local electric field and depends strongly on the arms handiness of the incident radiation. (c) Calculated CD spectra of LHPCM and RHPCM.

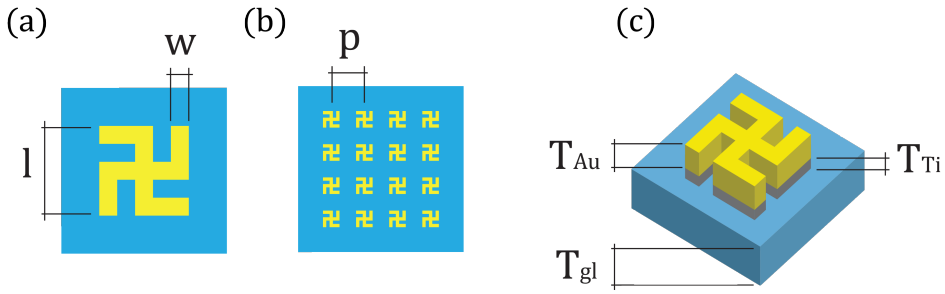

Figure 3. Design parameters of PCM. (a) Individual Gammadion parameters: l is the side of the square which contains the whole gammadion, and w is the width of the arms. (b) Distribution of gammadions into an Array, of pitch p. (c) T_{Au}, T_{Ti}, and T_{gl} are the thicknesses of gold, titanium, and glass respectively.

2.3. Nano fabrication

The PCM were made of gold on glass substrates with a thin adhesion layer of titanium. Figure 3 shows the design parameters of the gammadions. The initial parameters were $w = 80$ nm, $l = 400$ nm, $p = 800$ nm, $T_{Au} = 50$ nm, $T_{Ti} = 1$ nm and T_{gl} was fixed to 0.4 mm. Both, Right and Left handed PCM (RHPCM and LHPCM) were fabricated. The fabrication employs a negative lithography technique made using Electron Beam lithography (EBL). The successive steps of the fabrication process are briefly described below, and a schematic diagram of the successive step of the fabrication process is shown in the figure 4.

- First, evaporation of titanium and gold layers, using electron beam evaporation and thermal evaporation, respectively on $25 \times 25\,\mathrm{mm}^2$ glass substrates.

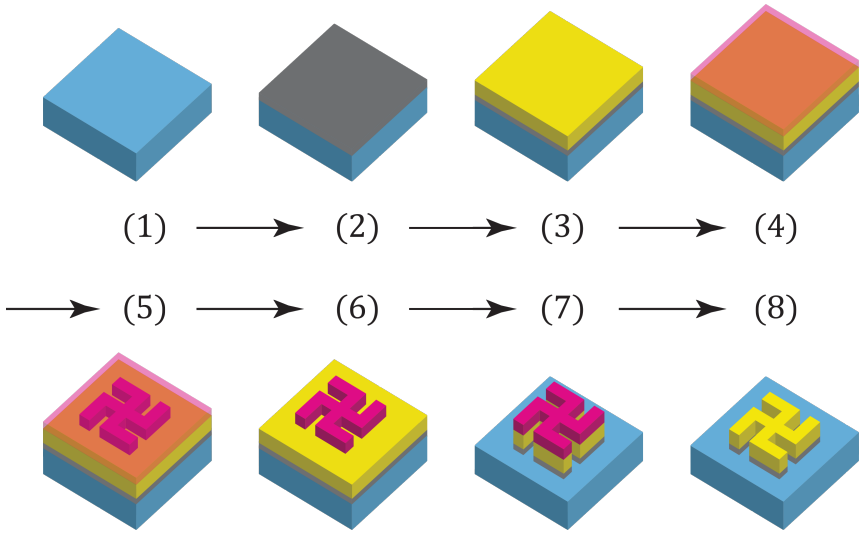

Figure 4. Negative lithography procedure. (1) Glass substrate, (2) Electron beam evaporation of titanium layer, (3) thermal evaporation of gold layer, (4) negative resist coating, (5) resist exposure, (6) resist development, (7) gold and titanium etch, and (8) resist etch.

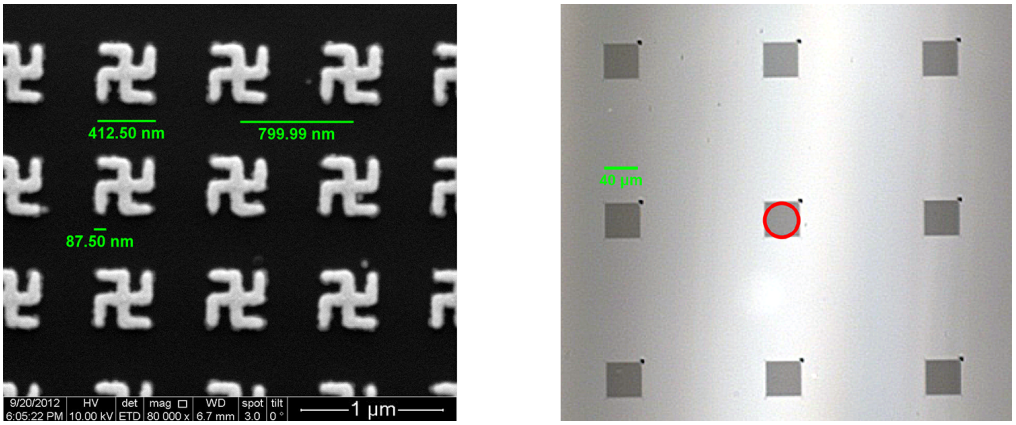

Figure 5. Left: SEM image of a portion of the fabricated gammadion array. Right: optical image showing the distribution of arrays. Each array is designed with different geometrical parameters. Collection area is marked with the red circle.

- Second, exposure of the design on samples coated by negative resist by 30 kV EBL.
- third, etching gold and titanium layers of developed sample by Argon plasma, followed by etching of resist by Oxygen plasma.

After fabricating the structures, their CD spectra were measured using the optical set-up, after were inspected with the Scanning Electron Microscope (SEM). Figure 5 shows a SEM image of fabricated structures and the corresponding optical image of the arrays on a sample, the size of each array (dark squares) coincide with the size of collection area.

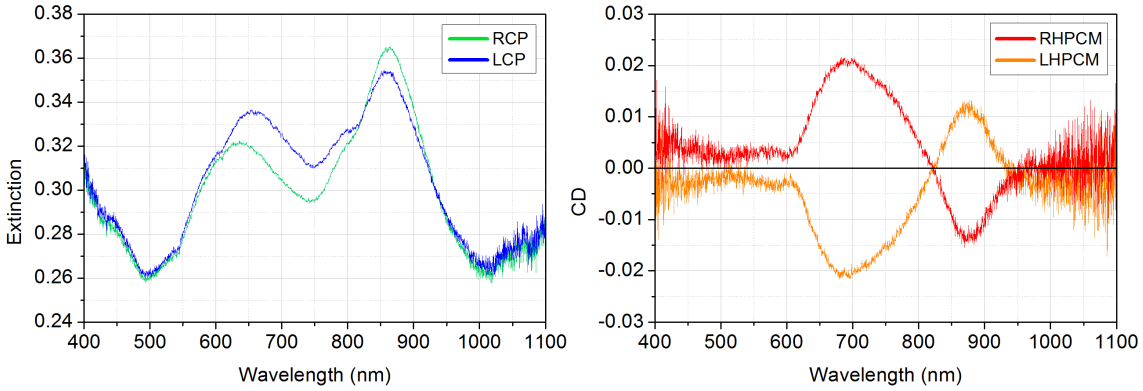

Figure 6. Left: Extinction of RHPCM using left and right circularly polarized light. Right: CD spectra of LHPCM and RHPCM. Gammadion's array parameters are $w = 80$ nm and $p = 800$ nm.

2.4. CD measurements

Experimentally we measured the extinction spectra of the fabricated nanostructures. The CD signal is proportional to the extinction difference:

$$CD \propto Ext_R - Ext_L \tag{2}$$

where

$$Ext = log(1 - T) = log(\frac{Ref - Bg}{Sig - Bg}) \tag{3}$$

where Ref is the transmitted signal throw the glass substrate, Bg is the background signal (mostly from the camera), and Sig is transmited signal throw the PCM [6].

3. Discusion

Once set up the optical platform, we worked on optimising the PCM structural parameters before testing them for molecular enantiomer discrimination.

3.1. Structure optimization

The main characteristic of chiral plasmonic nanostructures is their symmetric absorption for different handiness of circularly polarized light; while RHPCM absorbs more RCP light than LCP light (positive CD), LHPCM behaves the opposite way (negative CD), nevertheless this process is wavelength dependent and flips sign in different parts of the spectrum.

Figure 6 shows RCP and LCP extinction spectra for RHPCM and the CD spectra for RHPCM and LHPCM. Extinctions exhibit two pronounced peaks which are found to be sensitive to the handiness of the incident light (a). This translates into a non flat CD spectra (b). For seek of clarity only RCP extinction and CD of RHPCM is displayed.

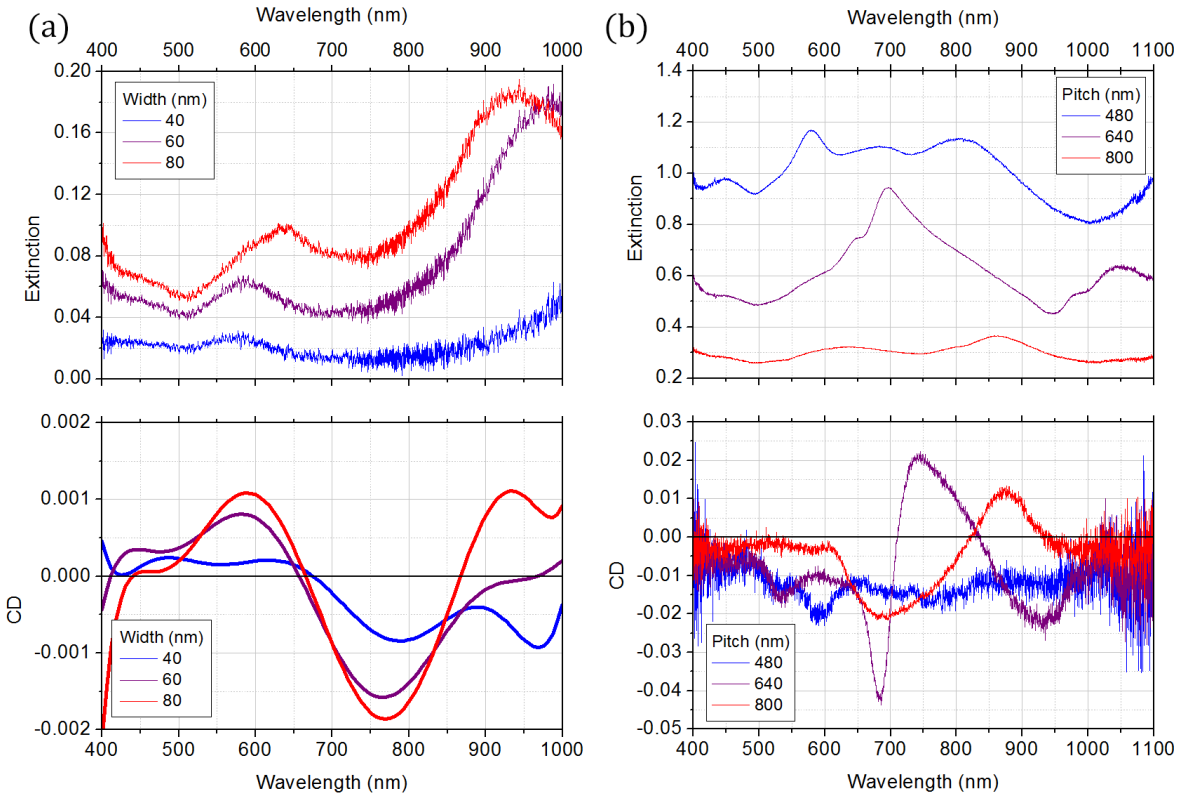

Figure 7. RCP Extinction and CD of RHPCM, (a) for varying width of the gammadion arms and (b) for different pitches.

First, we studied the influence on the extinction and CD spectra of gammadions arms width. Figure 7 (a) shows the extinction and CD spectra for a fixed pitch $p = 800$ nm. One can see how the extinction peak around 600 nm grows and shifts to longer wavelengths (red-shifted) when the width increases. Another peak comes from the Near Infrared Region (NIR) shifting to shorter wavelengths (blue-shifted). CD increases considerably with the width and its main lobes are situated around the extinction peaks.
We also studied the influence of the pitch of the gammadions array. The pitch between the gamadions was varied, maintaining the arm width constant to 80 nm. Figure 7 (b) shows how the extinction increases substantially when reducing the pitch. The overlap of the multiple peaks makes a further description of the trend difficult. Overall the associated CD gets sharper and more intense.
From these studies, we can deduce the best parameters for an optimum high signal over noise ratio and sharp CD features, two important features for sensing applications.

3.2. Molecule measurements

Preliminary measurements of the applicability of the PCM to discriminate between molecular enantiomers were performed on N-Isobutyryl-X-Cysteine (X=D or L specie).

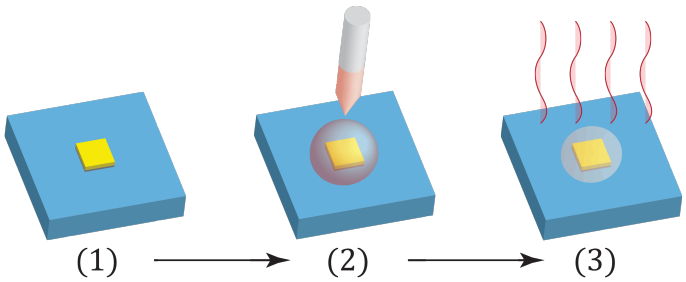

Figure 8. Schematic diagram of molecule deposition by evaporation process. (1) Sample with nanostructures arrays. (2) Molecule solution drop on the top of the structures. (3) Evaporation of the solvent and remaining molecule layer.

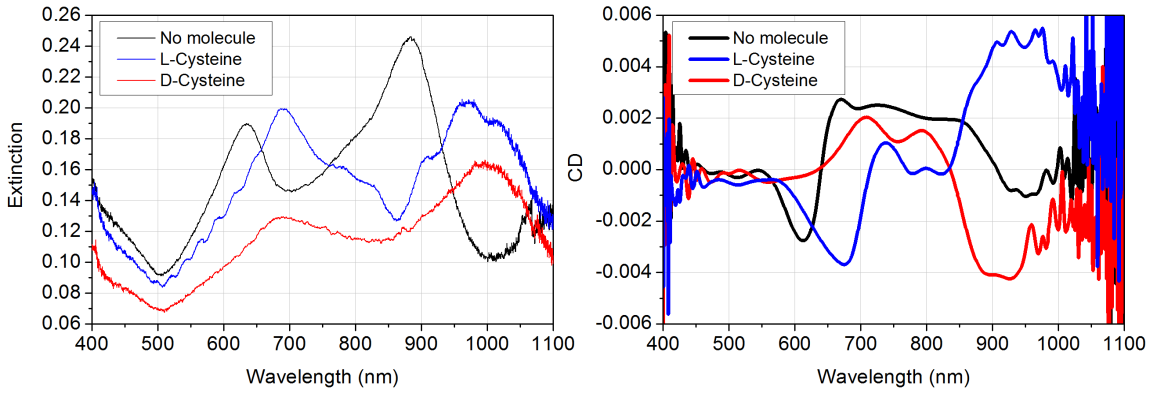

Figure 9. RCP Extinction and CD of RHPCM, of molecule measurements of L and D enantiomers of cysteine. Measurements were done with structures of parameters $w = 80$ nm and $p = 800$ nm. Left: Extinction. Right: CD.

Cysteine is a small molecule within a thiol group which has high affinity with gold [15]. From the previous study we chose a PCM with big signal to noise ratio and simple CD spectrum, to make easier on understanding of data. The PCM had 80 nm of arm width and 800 nm of pitch.

A drop of 10 μl of molecules in aqueous solution (concentration of 64 mg/ml, 335 mM) was deposited on the structures prior to evaporation at 30°C. Figure 8 shows a schematic of the deposition process.

A different sample was used for each of the cysteine enantiomers. The extinction and CD spectra of structure were measured before and after molecule deposition. Results are shown in figure 9.

Before molecule deposition, extinction exhibits two main peaks centred at 635 nm and 883 nm. After molecule deposition, the peak centred at 635 nm is red-shifted by 55 nm for both enantiomers, while the peak centred at 883 nm is red-shifted by 114 nm and 95 nm for D and L molecule respectively. This is consistent with the fact that both molecules have the same refractive index. The differences in the magnitude of the extinction peaks are attributed to the non-uniformty of the layer of molecules over the

sample, the thickness could change locally, however the layer is thick enough to cover all nanostructured area. The obtained CD signal changes are much more complex, importantly noticeable is the different change due to different molecule enantiomer. In particular, the originally negative peak at 609 nm shifts 67 nm in the presence of L molecules, while D molecules are supressing it. Additionally, the broad negative peak at 954 nm is enhanced in the case of D-molecules whereas L-molecules flip the sign.

4. Conclusion

An experimental set-up to measure circular dichroism was designed and built. This set-up allows the measurements on two dimensional planar chiral metamaterials samples. Once set up the optical platform, we optimize the PCM to display large and sharp circular dichroism signals. Preliminary experiments on chiral molecules were successfully conducted showing clear sensitivity to the two enantiomers.
At this stage, further control and understanding of plasmon enhanced CD measurements will require a better control of the molecular load. For this purpose we have already started to implement the PCM into a microfluidics environment.

5. Acknowledgements

I would like to thank Dr. Romain Quidant for his guidance and support during the development of the thesis.
I also thank Dr. Srdjan Acimovic, who performed numerical calculations of PCM, Dr. Jan Renger, for his help in the development of the experimental set-up, and his training in nanofabrication, Dr. Mark Kreuzer, for valuable discussions about the project.

6. References

[1] R. Quidant and M. Kreuzer. Biosensing: Plasmons offer a helping hand. *Nature Nanotec.*, 5(11):762–763, 2010.
[2] W. H. De Camp. The FDA perspective on the development of stereoisomers. *Chirality*, 1(1):2–6, 1989.
[3] D. L. Steinrnetz, W. G. Phillips, M. Wirick, and F. F. Forbes. A polarizer for the vacuum ultraviolet. *Appl. Opt.*, 6(6):1001–1004, 1967.
[4] O. Schnepp, S. Allen, and E. F. Pearson. The measurement of circular dichroism in the vacuum ultraviolet. *Rev. Sci. Instr.*, 41(8):1136–1141, 1970.
[5] S. A. Maier. *Plasmonics: fundamentals and applications.* Springer Science+ Business Media, 2007.
[6] S. Acimovic. *Localized surface plasmon resonance for biosensing Lab-on-a-Chip application.* ICFO-The institute of photonic sciences, 2012.
[7] A. O. Govorov, Z. Fan, P. Hernandez, J. M. Slocik, and R. R. Naik. Theory of circular dichroism of nanomaterials comprising chiral molecules and nanocrystals: plasmon enhancement, dipole interactions, and dielectric effects. *Nano Lett.*, 10(4):1374–1382, 2010.
[8] E. Hecht and A. Zajac. Optics. *4th Editon, Addison Wesley, San Francisco*, 2002.
[9] A. F. Drake. Polarisation modulation-the measurement of linear and circular dichroism. *J. Phys. E*, 19(3):170, 1986.

[10] N. A. Abdulrahman, Z. Fan, T. Tonooka, S. M. Kelly, N. Gadegaard, E. Hendry, A. O. Govorov, and M. Kadodwala. Induced chirality through electromagnetic coupling between chiral molecular layers and plasmonic nanostructures. *Nano Lett.*, 12(2):977–983, 2012.

[11] C. Gautier and T. Bürgi. Chiral n-isobutyryl-cysteine protected gold nanoparticles: preparation, size selection, and optical activity in the UV-VIS and infrared. *J. Am. Chem. Soc.*, 128(34):11079–11087, 2006.

[12] E. Hendry, T. Carpy, J. Johnston, M. Popland, R. V. Mikhaylovskiy, AJ. Lapthorn, S. M. Kelly, L. D. Barron, N. Gadegaard, and M. Kadodwala. Ultrasensitive detection and characterization of biomolecules using superchiral fields. *Nature Nanotech.*, 5(11):783–787, 2010.

[13] A. S. Schwanecke, A. Krasavin, D. M. Bagnall, A. Potts, A. V. Zayats, and N. I. Zheludev. Broken time reversal of light interaction with planar chiral nanostructures. *Phys. Rev. Lett.*, 91(24):247404, 2003.

[14] M. Kuwata-Gonokami, N. Saito, Y. Ino, M. Kauranen, K. Jefimovs, T. Vallius, J. Turunen, and Y. Svirko. Giant optical activity in quasi-two-dimensional planar nanostructures. *Phys. Rev. Lett.*, 95(22):227401, 2005.

[15] J. C. Love, L. A. Estroff, J. K. Kriebel, R. G. Nuzzo, G. M. Whitesides, et al. Self-assembled monolayers of thiolates on metals as a form of nanotechnology. *Chem. Rev.-Col.*, 105(4):1103–1170, 2005.